Bio-Inspired Thiolate-FeII-Hydrazine Adduct Towards Iron-Mediated C-N Bond Formation

Irene Cassandrini, Christian Philouze, Antoine Simonneau, Matthieu Koepf, Carole Duboc, Marcello Gennari

Bio-Inspired Thiolate-Fe^{II}-Hydrazine Adduct Towards Iron-Mediated C-N Bond Formation

Irene Cassandrini,[a] Christian Philouze,[a] Antoine Simonneau,[b] Matthieu Koepf,[c] Carole Duboc,[a] and Marcello Gennari*[a]

[a] I. Cassandrini, Dr. C. Philouze, Dr. C. Duboc, Dr. M. Gennari
Univ. Grenoble Alpes, CNRS UMR 5250, DCM
F-38000 Grenoble, France
E-mail: marcello.gennari@univ-grenoble-alpes.fr

[b] Dr. A. Simonneau
LCC-CNRS, Université de Toulouse, CNRS, UPS
205 route de Narbonne, BP44099, 31077 Toulouse cedex 4 (France)

[c] Dr. M. Koepf
Univ. Grenoble Alpes, CNRS, CEA, IRIG, LCBM
17 rue des Martyrs, Grenoble F-38000, France.

Supporting information for this article is given via a link at the end of the document.

Abstract: The bio-inspired dinuclear iron(II) complex $[Fe^{II}(L)]_2$ (L^{2-} = 2,2'-(2,2'-bipyridine-6,6'-diyl)bis(1,1'-diphenylethanethiolate)), featuring alkyl thiolate ligands, was found to react with hydrazine (N_2H_4) to form an unprecedented alkyl thiolate-supported Fe^{II}-N_2H_4 adduct, $[LFe^{II}(N_2H_4)]$. This complex was characterized structurally by X-ray crystallography, spectroscopically (^{1}H NMR, UV-vis, IR), and electrochemically. Unexpectedly, in CH_3CN solution, $[LFe^{II}(N_2H_4)]$ gradually evolved to yield an Fe^{II}-acetohydrazonohydrazide complex, $[LFe^{II}(H_2N_2C(CH_3)N_2H_3)]$, the C-N bond formation resulting from the reaction between N_2H_4 and CH_3CN mediated by the Fe^{II} ion. Its structure, confirmed by X-ray diffraction on single crystals, reveals a η¹-coordination of the acetohydrazonohydrazide ligand. The proposed mechanism is based on the electrophilic activation of a CH_3CN molecule by Fe^{II}, followed by the nucleophilic attack of a free hydrazine. This work expands the reactivity landscape of iron-hydrazine complexes and provides new insights into potential pathways for N-N bond functionalization in nitrogen fixation processes.

Introduction

Nitrogenase enzymes[1] are a source of inspiration in the pursuit of efficient and mild artificial fixation of dinitrogen (N_2) into ammonia (NH_3).[2] In Mo-nitrogenases, the FeMo cofactor (FeMo-co) catalyzes NH_3 evolution at ambient temperature and pressure from N_2, protons, electrons, and ATP.[1c]
The substrate activation by FeMo-co is proposed to occur at a dinuclear iron unit within a sulfide-rich environment.[3] Furthermore, the reduction of N_2 is suggested to proceed via an *alternating* pathway involving hydrazine (N_2H_4) as an intermediate. This is supported by (i) the ability of nitrogenases to process N_2H_4 as a substrate,[1d] (ii) the freeze-trapping of a common intermediate in MoFe protein variants using either diazene (N_2H_2) or hydrazine as a substrate,[4] (iii) the N_2H_4 release upon acid or base quenching of Mo-nitrogenase during N_2 reduction,[5] and (iv) the N_2H_4 detection as an intermediate in N_2 reduction by alternative nitrogenases.[6]
Inspired by nitrogenases and in the search for efficient artificial nitrogen fixation systems, bioinorganic chemists have focused on isolating sulfur-rich, low-nuclearity iron complexes and studying their reactivity with N_2 and related substrates.[7] In this context, while a variety of iron-hydrazine complexes have been reported[8] (28 entries in the CCDC database, mostly supported by phosphine co-ligands), examples featuring the biologically relevant sulfur ligation are relatively scarce (Scheme 1).[9] These complexes predominantly feature aryl thiolates as supporting ligands,[9a-c, 9e] while only a single example features a bridging sulfide[9d] as found in FeMo-co. These sulfur-rich Fe-N_2H_4 complexes exhibit diverse structural features, with iron invariably in the +2 oxidation state. While the mononuclear species include terminally bound N_2H_4 (Scheme 1, left),[9a-c] the dinuclear complexes feature a μ-η¹:η¹-N_2H_4 bridging mode (Scheme 1, right).[9d, 9e] Curiously, no examples of Fe-N_2H_4 complexes supported by aliphatic thiolates, which better mimic bridging sulfides than aryl thiolates, have been reported to date.

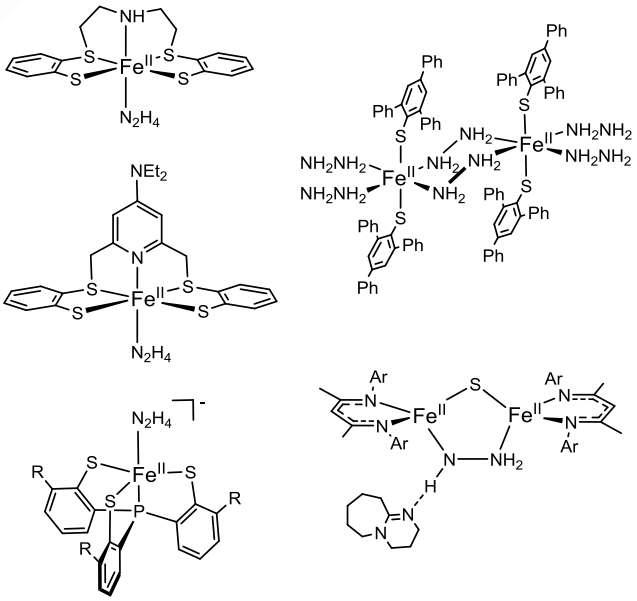

Scheme 1. Previously reported iron-hydrazine complexes supported by sulfur-based ligands.

To address this gap, we report here the reactivity of two dinuclear Fe-alkylthiolate complexes with hydrazine. These complexes, $[Fe^{II}(L)]_2$ (**Fe_2^S**)[10] and $[Fe^{II}{}_2(LSSL)]^{2+}$ (**Fe_2^{SS}**),[11] have

been previously reported by our group (Scheme 2, L^{2-} = 2,2'-(2,2'-bipyridine-6,6'-diyl)bis(1,1'-diphenylethanethiolate, $LSSL^{2-}$ is the disulfide form of L^{2-}). Notably, **Fe_2^S** and **Fe_2^{SS}** feature diiron units within a sulfur-rich environment reminiscent of the N_2-activation site in the FeMo-co.[3] The present study led to generate the first alkyl thiolate-supported Fe-N_2H_4 complex, [$LFe^{II}(N_2H_4)$] (**Fe^{N2H4}**). Surprisingly, over time in CH_3CN solution, we observed the progressive formation of an Fe^{II}-acetohydrazonohydrazide adduct (Scheme 2), resulting from the formation of two C-N bonds between N_2H_4 and CH_3CN in an Fe^{II}-mediated process. This unexpected reactivity expands the potential of hydrazine-based transformations in synthetic organometallic chemistry and sheds light on possible N–N bond functionalization pathways in nitrogen fixation processes.

Results and Discussion

1. Reactivity of two dinuclear Fe^{II}-thiolate complexes with hydrazine

1.1. Fe^{II} precursors

The two previously reported dinuclear Fe^{II}-thiolate complexes, $[Fe^{II}(L)]_2$ (**Fe_2^S**)[10] and $[Fe^{II}{}_2(LSSL)]^{2+}$ (**Fe_2^{SS}**)[11] (Scheme 2), were employed as precursors for reactivity studies with N_2H_4. **Fe_2^{SS}** is the 2-electron oxidized form of **Fe_2^S**, with the oxidizing equivalents stored in a disulfide unit.

The synthetic procedure for **Fe_2^S** was scaled up and slightly modified in the work-up compared to the reported procedure.[10] Conversely, **Fe_2^{SS}** was isolated by an alternative, more convenient two-step route compared to our previous report.[11] This method involves the generation of [$LFe^{III}Cl$][12] followed by chloride metathesis in the presence of $NaBAr^F{}_4$ in CH_2Cl_2. This process induces dimerization, forming **Fe_2^{SS}** through the reduction of Fe^{III} to Fe^{II} and the simultaneous oxidation of two thiolates to a disulfide bond.

It is important to note that in CH_3CN solution, **Fe_2^{SS}** exists in equilibrium with a mononuclear [$LFe^{III}(CH_3CN)]^+$ species, as previously demonstrated.[11] Similarly, variable-temperature ^{1}H NMR measurements on **Fe_2^S** in CD_3CN (Figure S1 of the Supporting Information) reveal fluxionality, attributed to a rapid exchange between **Fe_2^S** and the corresponding mononuclear CH_3CN adduct, [$LFe^{II}(CH_3CN)$]. The dynamic nature of these complexes in solution has an impact on their reactivity, as discussed in the following sections.

1.2. Spectroscopic monitoring of the reactivity with N_2H_4

In CH_3CN solution, 20 equiv. of hydrazine (N_2H_4) vs. Fe were added to both **Fe_2^S** and **Fe_2^{SS}** (Scheme 2). Indeed, an excess of N_2H_4 (typically ≥ 3–5 equivalents) is commonly added to metal precursors due to its weak coordination abilities.[9a, 9c, 13]

UV-vis absorption spectroscopy was used to monitor the reaction progress under diluted conditions (Figure 1). Starting with **Fe_2^S**, the spectrum showed only slight changes after a few minutes, with the main absorption band shifting from 624 nm to 635 nm (ε ≈ 3400 $M^{-1}{\cdot}cm^{-1}$).

When starting from **Fe_2^{SS}**, we observed both (i) the progressive disappearance of the thiolate to Fe^{III} LMCT band at 449 nm, characteristic of [$LFe^{III}(CH_3CN)]^+$,[11] indicating the reduction of Fe^{III} to Fe^{II}, and (ii) the formation of the aforementioned product with a band at 635 nm.

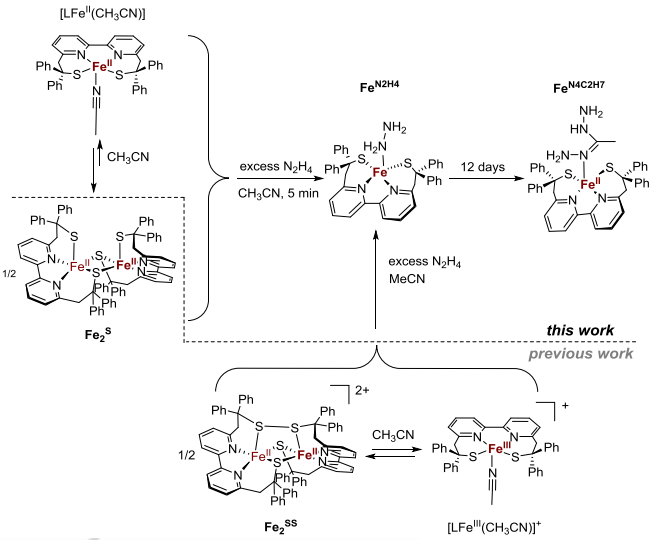

Scheme 2. Summary of the reactivity described in this paper.

The observation of the same primary adduct, regardless of the starting complex (**Fe_2^S** or **Fe_2^{SS}**), suggests that the N_2H_4 excess acts as a reducing agent towards the oxidized form of the complex ([$LFe^{III}(CH_3CN)]^+$ and/or **Fe_2^{SS}**).

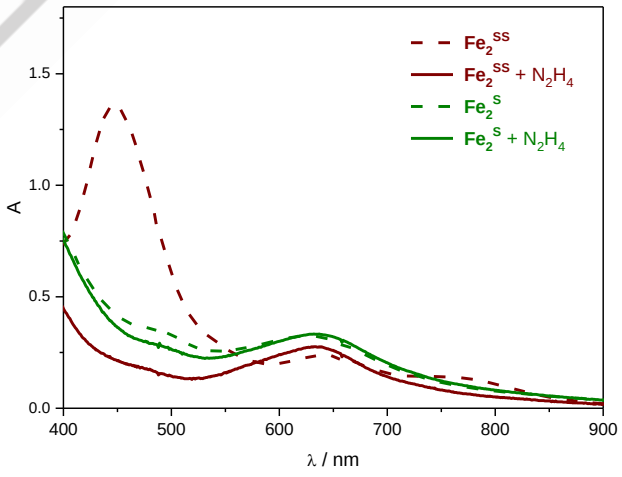

Figure 1. 4 UV−vis absorption spectra of **Fe_2^S** (red) and **Fe_2^{SS}** (black) (~0.1 mM solutions, 1 cm path length) in CH_3CN before (dotted line) and after (solid line) the addition of 20 equiv. N_2H_4 ad[14]dition (10 min reaction).

^{1}H NMR monitoring confirmed these conclusions. Specifically, regardless of the employed precursor, a few minutes after the addition of hydrazine, the same paramagnetic product is observed in the ^{1}H NMR spectrum, with two peaks at 69.9 and 55.0 ppm (Figure 2a, dark red spectrum, and Figure S2). This species is attributed to a mononuclear Fe^{II}-N_2H_4 adduct, [$LFe^{II}(N_2H_4)$] (**Fe^{N2H4}**, see next section). It should be noted that

when starting from **Fe_2^{SS}**, an additional paramagnetic product with peaks in the 52-16 ppm region is discernible. It does not correspond to **Fe_2^{S}** or its protonated form, and its identity remains uncertain.

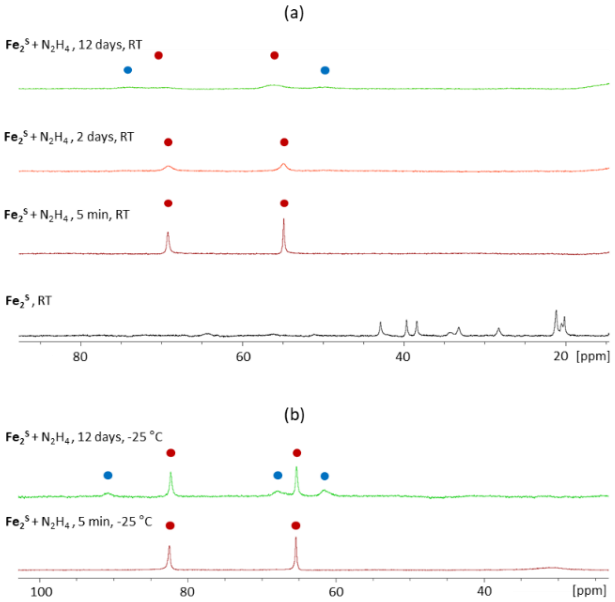

Figure 2. Paramagnetic region of the ^{1}H NMR spectra of **Fe_2^{S}** in CD_3CN before and after addition of 20 equiv. N_2H_4 at different times (a) at room temperature vs. (b) at low temperature (-25 °C). Red circles indicate peaks attributed to **Fe^{N2H4}**, while blue circles those to **Fe^{N4C2H7}**.

1.3. Isolation and solid state characterization of the Fe^{II}-N_2H_4 adduct

The aforementioned mononuclear Fe^{II}-N_2H_4 adduct, $[LFe^{II}(N_2H_4)]$ (**Fe^{N2H4}**) could be isolated as a dark green precipitate formed after 5 min from a concentrated **Fe_2^{S}** - N_2H_4 (20 equiv.) mixture in acetonitrile. The product was identified by elemental analysis and solid-state IR spectrum (Figure S3), exhibiting peaks in the 3150-3300 cm^{-1} region, characteristic of N-H stretching vibrations of metal-bound N_2H_4.[15]

Single crystals could be grown over one week by vapor diffusion of pentane into the mother liquor. Surprisingly, at this longer timescale the corresponding structure reveals two chemically independent molecules in the asymmetric unit: $[LFe^{II}(N_2H_4)]$ (**Fe^{N2H4}**) (Figure 3a) and a secondary product, $[LFe^{II}(H_2N_2C(CH_3)N_2H_3)]$ (**Fe^{N4C2H7}**) (Figure S4), the latter of which will be discussed in detail in section 2.1. Crystallographic data on $[LFe^{II}(N_2H_4)]\cdot[LFe^{II}(H_2N_2C(CH_2)N_2H_3)]$ (**Fe^{N2H4}•Fe^{N4C2H7}**), including selected bond lengths and angles, are summarized in Tables S1-S3 in the Supporting Information.

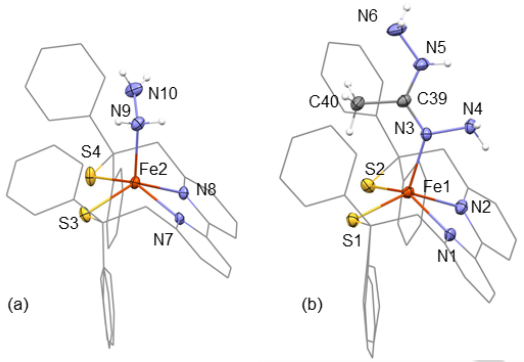

Figure 3. Molecular structure of (a) the **Fe^{N2H4}** unit from **Fe^{N2H4}**·**Fe^{N4C2H7}**, and (b) pure **Fe^{N4C2H7}**, as determined by single-crystal X-ray diffraction. The thermal ellipsoids of the metal cores are drawn at 30% probability level. All hydrogen atoms of L^{2-} and solvent molecules are omitted for clarity.

We attribute the adduct detected by ^{1}H NMR after a few minutes of reaction (Figure 2a, peaks indicated by red circles) to the **Fe^{N2H4}** unit of **Fe^{N2H4}**•**Fe^{N4C2H7}**. This complex displays a pentacoordinated Fe^{II} center in an N_3S_2 environment, with a basal N_2S_2-multidentate L^{2-} ligand and an apical η^1-N_2H_4 co-ligand**.** The coordination geometry is distorted square pyramidal (τ_5 = 0.08),[16] with the metal ion displaced 0.644 Å from the N_2S_2 plane defined by the L^{2-} ligand. The Fe-$N_{hydrazine}$ distance of 2.142 Å falls within the typical range for terminal Fe^{II}-bound hydrazine complexes. Notably, the hydrazine hydrogen atoms engage in weak hydrogen bonding interactions with sulfur atoms of the second independent **Fe^{N4C2H7}** unit (N···S distances of 3.371(5) and 3.432(6) Å).

Previously reported iron(II)-hydrazine complexes supported by sulfur ligands (including aryl thiolates, thioethers, and sulfides, but not alkyl thiolates, see Scheme 1) exhibit different nuclearities (mononuclear or dinuclear) and coordination geometries (tetrahedral, trigonal bipyramidal, or octahedral), and can display both terminal (η^1) and bridging ($\mu_{1,2}$) coordination modes for hydrazine, with no significant discrepancies in Fe-N distances (ranging from 2.036 to 2.231 Å for terminal and 2.164 to 2.227 Å for bridging N_2H_4). In the present study, we could exclusively isolate the η^1-N_2H_4 adduct **Fe^{N2H4}** with aliphatic thiolate ligands. Attempts to isolate a bridging Fe^{II}-N_2H_4-Fe^{II} species with a Fe:N_2H_4 ratio of 2:1 were unsuccessful. The potential instability of such LFe^{II}-N_2H_4-$Fe^{II}L$ adduct can be attributed to either (i) steric hindrance from the phenyl groups of L^{2-}, preventing the bridging coordination of the six-atom N_2H_4 ligand, or (ii) the weaker coordination ability of the $N_2N_{N2H4}{}^bS_2$ donor set (*b* = bridging) compared to the N_2S_3 donor set in **Fe_2^{S}**.

1.4. Electrochemical properties

The redox properties of **Fe^{N2H4}** were explored through cyclic voltammetry (CV). The CV of **Fe_2^{S}** was recorded in CH_3CN 0.1 M *n*-Bu_4NPF_6 before and after adding 10 equiv. of N_2H_4, and compared to the CV of free N_2H_4.

For **Fe_2^{S}**, a reversible peak attributed to the Fe^{II}/Fe^{III} redox couple is observed at $E_{1/2}$ = -0.58 V vs Fc^+/Fc, as previously reported.[10] Upon the addition of N_2H_4, this peak shifted cathodically to $E_{1/2}$ = -0.68 V (ΔE_p = 54 mV), maintaining its

reversibility. The 100 mV cathodic shift is consistent with a more electron-rich coordination environment around Fe^{II} in the presence of N_2H_4, changing from $N_2S^tS_2^b$ in **Fe_2^S** to $N_2N^{N2H4}S_2^t$ in **Fe^{N2H4}** (*t* = terminal, *b* = bridging).

The preserved reversibility of the Fe^{II}/Fe^{III} system in the presence of N_2H_4 suggests that the electrogenerated Fe^{III}-N_2H_4 species is stable on the CV timescale. However, over a longer timescale, the excess hydrazine reduces back Fe^{III} to Fe^{II}, as described for the reaction of $[LFe^{III}(CH_3CN)]^+$ with N_2H_4 in section 1.2.

The onset of the irreversible oxidation peak for free N_2H_4, at around -0.3 V, remains unaffected by the presence of **Fe_2^S**. This indicates that the **Fe_2^S/Fe^{N2H4}** system does not exhibit catalytic activity towards N_2H_4 oxidation under these conditions.

To our knowledge, this study presents the first electrochemical data for iron-sulfur-N_2H_4 adducts, providing a valuable benchmark for future studies in the field of bio-inspired iron-sulfur chemistry with relevance to nitrogen fixation.

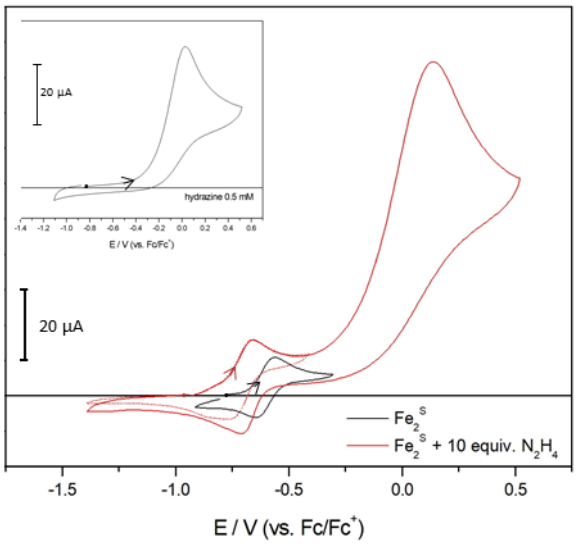

Figure 4. CVs of 0.5 mM solutions (CH_3CN 0.1 M *n*-Bu_4NPF_6) of **Fe_2^S** before (black line) and after addition of 5 equiv. N_2H_4 (red line), compared to the CV of free N_2H_4 (inset). GC working electrode, $Ag/AgNO_3$ reference electrode, Pt wire counter electrode, 100 $mV{\cdot}s^{-1}$.

2. Iron-mediated reactivity of hydrazine with acetonitrile

2.1. Generation and characterization of a Fe^{II}-acetohydrazonohydrazide complex

When monitoring the reaction of **Fe_2^S** with 20 equiv. of N_2H_4 by ^1H NMR in CD_3CN at room temperature (Figure 2a), we observed the slow appearance (in the timescale of days) of a secondary paramagnetic product displaying very broad signals at ~50, and ~74 ppm, in addition to **Fe^{N2H4}**.[17] When the spectrum is registered at -25 °C (Figure 2b), fluxionality is suppressed, and three more defined peaks, at 95.9, 71.9, and 65.9 ppm, can be assigned to the same species. We propose to assign this species to the acetohydrazonohydrazide adduct $[LFe^{II}(H_2N_2C(CH_3)N_2H_3)]$ (**Fe^{N4C2H7}**), co-crystallized with **Fe^{N2H4}** in **Fe^{N2H4}•Fe^{N4C2H7}** (see section 1.3). When a CH_3CN solution of **Fe_2^S** was exposed to 20 equiv. of N_2H_4 and subsequently filtered, single crystals of pure **Fe^{N4C2H7}** could be obtained by diffusing diethyl ether over three weeks (Figure 3b, Tables S1-S3).

The X-ray diffraction structures of pure **Fe^{N4C2H7}** and the **Fe^{N4C2H7}** unit within **Fe^{N2H4}•Fe^{N4C2H7}** exhibit very high similarity. For simplicity, we thus focus on the structure resolved from a crystal of pure **Fe^{N4C2H7}**. It reveals the apical coordination of a planar acetohydrazonohydrazide molecule to Fe^{II} via a nitrogen atom in α-position to the central carbon atom (Scheme 3).

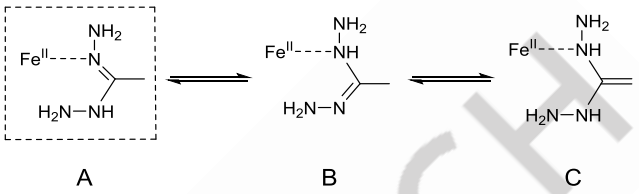

Scheme 3. Tautomeric forms of Fe^{II}-bound acetohydrazonohydrazide.

The pentacoordinated, distorted square pyramidal geometry around Fe^{II} (τ_5 = 0.04)[16] is completed by the coordination of the L^{2-} ligand in the basal plane. The coordinated co-ligand is primarily attributed to tautomer A depicted in Scheme 3, although contributions from the other tautomers could not be excluded. This assignment is supported by (i) the identification of electron density corresponding to three hydrogen atoms around C(40), (ii) a C(39)–C(40) distance of 1.496(5) Å consistent with a C_{sp^2}–C_{sp^3} single bond, and (iii) a slight difference in the C(39)–N(3) and C(39)–N(5) bond lengths (1.300(4) vs. 1.331(4) Å). The C(39) angle of 121.7(3)° indicates its sp^2 hybridization. As for **Fe^{N2H4}**, the hydrazine hydrogen atoms are involved in weak H-bonding interactions with sulfur atoms (N···S distances of 3.452(4) and 3.547(3) Å).

2.2. Discussion on the N_2H_4- CH_3CN coupling and proposed mechanism

Classically, the reaction between hydrazines and nitriles requires the electrophilic activation of the nitrile by the presence of a Lewis acid like $AlCl_3$.[18] However, while transition-metal (TM) promoted nucleophilic addition of alcohols, amines, and water to coordinated nitriles is well documented,[18] examples of analogous TM-mediated reactivity with the weak nucleophile hydrazine are limited to two examples.[13a, 19]

A family of phosphite-supported Fe^{II}-nitrilehydrazine complexes was reported to be unstable in solution and gradually transform into amidrazone complexes, including a five-membered metallacycle.[13a] Amidrazones (RC(=NH)$NHNH_2$) arise from the monosubstitution of a nitrile by a single hydrazine molecule. Mechanistically, a nucleophilic attack by one terminal nitrogen of NH_2NH_2 on the cyanide carbon of the Fe-coordinated nitrile was proposed.

Additionally, a palladium(II)-NHC complex was shown to generate a Pd-acetohydrazonohydrazide adduct in the presence of an excess of N_2H_4 in CH_3CN solution.[19] Unlike the previous case, this palladium-mediated transformation was proposed to involve the sequential nucleophilic attack of two Pd-coordinated N_2H_4 molecules with free CH_3CN. The intramolecular nature of the second step, leading to the formation of a five-membered

metallacycle, was proposed to be likely the driving force for the overall reaction.

Concerning our iron-based system, in the attempt to propose a reaction mechanism, the following aspects should be considered:

- We suggest that a small amount of the mononuclear [LFe^{II}(CH$_3$CN)] species (see Section 1.1) persists in CH$_3$CN solution even upon the addition of an excess of the weakly coordinating N$_2$H$_4$.
- The phenyl rings of the N$_2$S$_2$ ligand impose a spatial constraint, favoring pentacoordination[10-11, 20] over hexacoordination[21] and preventing *cis*-coordination of N$_2$H$_4$ and CH$_3$CN within the same species.
- The monodentate coordination of acetohydrazonohydrazide in the final product **Fe^{N4C2H7}** rules out a five-membered metallacycle as the driving force behind the process, unlike what was observed in previous examples.

Considering these points and knowing that Fe^{II}, as a Lewis acid, can electrophilically activate CH$_3$CN and decrease the nucleophilicity of N$_2$H$_4$, a reaction mechanism is proposed in Scheme 4.

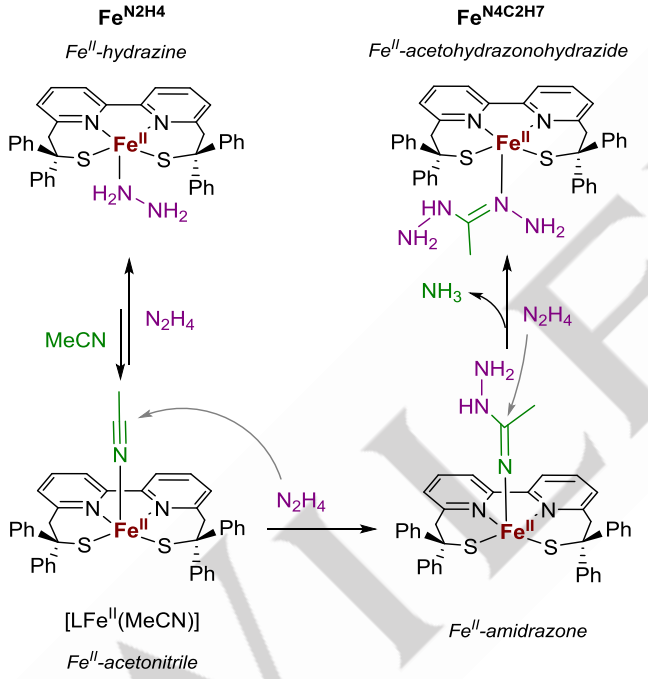

Scheme 4. Proposed mechanism for Fe^{II}-mediated C-N bond formation between N$_2$H$_4$ and CH$_3$CN.

In this pathway, a small amount of [LFe^{II}(CH$_3$CN)], in rapid equilibrium with **Fe^{N2H4}**, undergoes nucleophilic attack by a free hydrazine on the Fe^{II}-activated cyanide moiety. This results in the formation of a Fe^{II}-amidrazone complex, which can subsequently react with a second equivalent of N$_2$H$_4$ to generate the final **Fe^{N4C2H7}** product and one equivalent of ammonia. Interestingly, ammonia could be detected and quantified by ion chromatography (see experimental section), enabling the estimation of an ~18% yield (based on Fe) for the Fe-driven formation of acetohydrazonohydrazide after 12 days.

Experimental Section

General methods. The ligand H$_2$L, i.e. the diprotic form of (2,2'-(2,2'-bipyridine-6,6'-diyl)bis(1,1'-diphenylethanethiolate)),[12] as well as the [Fe$^{II}_2$(L)(LH)]BF$_4$[20d] and of [LFe^{III}Cl][12] precursors, were prepared as described previously. The synthesis of [Fe^{II}(L)]$_2$ (**Fe$_2^S$**)[10] and [Fe$^{II}_2$(LSSL)]$^{2+}$ (**Fe$_2^{SS}$**)[11] complexes was modified from published procedures and conducted under a dry nitrogen atmosphere in a glovebox (< 5 ppm O$_2$, < 10 ppm H$_2$O). All glassware was oven-dried before use, and reagents were employed as received. Solvents were distilled under argon over Na/benzophenone (THF, Et$_2$O, pentane, with 1% diglyme for pentane) or CaH$_2$ (CH$_3$CN, CH$_2$Cl$_2$), degassed, and stored in the glovebox over activated 3 Å molecular sieves.

Paramagnetic ^{1}H NMR spectra were recorded on Bruker Avance III 400 or 500 MHz spectrometers. Chemical shifts are reported in ppm relative to tetramethylsilane, using the solvent residual peak of CD$_2$Cl$_2$ (δH 5.32) or CD$_3$CN (δH 1.94) as a reference. Deuterated solvents were dried with CaH$_2$ or activated 3 Å molecular sieves before use.

UV-Vis spectra were obtained on a Cary 300 spectrophotometer using a 1 cm quartz cuvette. Infrared spectra were collected on a Thermo Scientific Nicolet iS10 FT-IR spectrometer equipped with ATR or transmission modules.

Crystal structure determination. Single crystal X-ray diffraction was performed using a Nonius-Bruker 4-circle diffractometer with an APEXII CCD detector. Mo Kα radiation (λ = 0.71073 Å) was monochromatized by multilayer mirrors from an Incoatec high brilliance microsource. Data were collected at 200 K with samples mounted in inert oil.

Cell refinement, integration, absorption correction, and data reduction were carried out using Eval, Sadabs, and Xprep (Nonius-Bruker). Structures were solved by intrinsic phasing methods and refined on F^2 using full matrix least-squares techniques with SHELXL.[22] implemented in Olex2.Non-hydrogen atoms were refined anisotropically; hydrogen atoms were placed geometrically and constrained to ride on their carrier atoms.

Structures were deposited with CCDC numbers 2379804 and 2379805 for **Fe^{N2H4}•Fe^{N4C2H7}** and for **Fe^{N2H4}** respectively and can be obtained free of charge from the Cambridge Crystallographic Data Centre via www.ccdc.cam.ac.uk/data_request/cif.

Electrochemistry. Cyclic voltammetry experiments were conducted in argon-saturated CH$_3$CN (<5 ppm O$_2$) using tetrabutylammonium hexafluorophosphate (*n*-Bu$_4$NPF$_6$) as the supporting electrolyte. A PGSTAT100N Metrohm-Autolab potentiostat/galvanostat was used with a standard three-electrode cell. Potentials were referenced to Ag/0.01 M AgNO$_3$ in CH$_3$CN + 0.1 M *n*-Bu$_4$NPF$_6$ and calibrated using an internal Fc$^+$/Fc standard. The working electrode was a glassy carbon electrode (3 mm diameter) polished with 2 µm diamond paste. A Pt rod served as the auxiliary electrode. Cyclic voltammograms

were recorded at 100 mV/s scan rate. Anodic (Ep_a) and cathodic (Ep_c) peak potentials were measured, with $E_{1/2} = (Ep_a + Ep_c)/2$ and $\Delta E_p = Ep_a - Ep_c$.

Synthesis of $[Fe^{II}L]_2$ (**Fe_2^S**). This procedure is adapted from a previously reported method.[10] To a suspension of $[Fe^{II}_2(L)(LH)]BF_4$ (120 mg, 0.087 mmol) in CH_3CN (4 mL) at 293 K, NaH (60% in mineral oil, 4 mg, 0.098 mmol) was added under stirring. The reaction mixture was stirred for 3 hours, during which the color changed from dark grey to dark green. The resulting mixture was filtered, and the solid residue was extracted with CH_3CN:THF (1:1, 3 mL x 4). All the filtrates were combined and, after solvent evaporation under vacuum, the resulting solid was washed with CH_3CN (2 x 2 mL), filtered, and dried to yield **Fe_2^S** as a dark green powder (43 mg, 0.034 mmol, 80% yield). The ^{1}H NMR spectrum differs from the previously published one,[10] which is now attributed to a hydrolysis product generated from **Fe_2^S** in the presence of traces of moisture. ^{1}H NMR (400 MHz, CD_3CN, 293 K): δ 64.42, 56.10, 42.88, 39.64, 38.38, 33.27, 28.30, 21.17, 20.25, 13.06, 11.78, 11.14, −1.28. UV-Vis. (CH_3CN, 298 K, nm {$M^{-1}cm^{-1}$}): 313 {18400}, 491 {3550}, 630 {2800}. Other characterization data for this compound have been previously reported.

Synthesis of $[Fe^{II}_2(LSSL)](BAr^F)_2$ (**Fe_2^{SS}**). [$LFe^{III}Cl$] (161 mg, 0.24 mmol) was dissolved in CH_2Cl_2 (5 mL) to afford a dark brown suspension. A solution of $NaBAr^F_4$ (235 mg, 0.27 mmol) in Et_2O (2 mL) was added and after stirring for 15 min a dark orange mixture was obtained. The generated NaCl was filtered off, and the filtrate was concentrated under vacuum. The product was precipitated by addition of excess hexane, filtered, washed with hexane, dried, and collected as a dark orange powder (289 mg, 0.10 mmol, 82%). The characterization data for the $[Fe^{II}_2(LSSL)]^{2+}$ cation of this $BAr^F_4^-$ salt are consistent with those previously reported for the corresponding ClO_4^- salt.[11]

Synthesis of $[LFe^{II}(N_2H_4)]$ (**Fe^{N2H4}**). Hydrazine (0.38 mL, 1.0 M in THF, 0.38 mmol) was added to a dark green suspension of **Fe_2^S** (24.0 mg, 0.019 mmol) in acetonitrile (2 mL). The reaction mixture immediately turned dark green-bluish and was stirred at room temperature. After 5 min, a dark green precipitate formed, which was filtered, washed with acetonitrile (1 mL), dried and collected. (12.7 mg, 0.019 mmol, 50%).

Anal. Calcd for $C_{38}H_{30}N_2S_2FeN_2H_4 \cdot 0.4H_2O \cdot 0.4C_4H_8O$ (702.73): C, 67.68; H, 5.45; N, 7.97; S, 9.13. Found: C, 67.54; H, 5.31; N, 7.96; S, 9.13. IR (ATR, cm^{-1}): 3309 (w, νN-H), 3226 (w, νN-H), 3133 (w, νN-H), 3054 (w), 3014 (w), 2912 (w), 1595 (s), 1564 (m), 1484 (s), 1458 (m), 1441 (s), 1392 (w), 1322 (w), 1282 (w), 1265 (w), 1173 (s), 1084 (m), 1027 (m), 1010 (m), 966 (m), 905 (m), 853 (w), 778 (s), 752 (s), 678 (s), 667 (s), 640 (m).

Cristallization of $[LFe^{II}(N_2H_4)][LFe^{II}(H_2N_2C(CH_2)N_2H_3)]$ (**Fe^{N2H4}·Fe^{N4C2H7}**) *and* $[LFe^{II}(H_2N_2C(CH_3)N_2H_3)]$ (**Fe^{N4C2H7}**). **Fe_2^S** (3 mg) was dissolved in CH_3CN (1 mL) to obtain a dark green suspension. Upon addition of 20 equiv. hydrazine, the reaction mixture turned into an emerald green solution. After one day the mixture was filtered, and black single crystals corresponding to **Fe^{N2H4}•Fe^{N4C2H7}** were obtained by vapor diffusion of pentane (poorly miscible with CH_3CN) over one week. When the same procedure was repeated, but vapor diffusion was carried out with diethyl ether, black single crystals corresponding to pure **Fe^{N4C2H7}** were obtained after three weeks.

Detection of NH_4^+ *by Ion Chromatography.* To analyze $NH4^+$ formation, the reaction was repeated using **Fe_2^S** (7.5 mg, 0.006 mmol) and hydrazine (0.12 mL, 1.0 M in THF, 0.12 mmol, 20 equiv.) in acetonitrile (5 mL). After stirring for 12 days in the dark, H_2SO_4 (5 mL, 0.2 M in Milli-Q water) was added to convert NH_3 to $NH4^+$. The mixture was filtered through a 0.45 µm PTFE syringe filter and diluted to 50 mL with Milli-Q water to afford sample *S* (see Table S3). Two control experiments were performed: (*C1*) prepared following the same procedure but omitting the addition of **Fe_2^S**, and (*C2*) identical to *C1* but quenched with H_2SO_4 after 1 min instead of 12 days. For each sample, two independent batches were prepared and analyzed in duplicate.

Ion chromatograms were recorded on a Metrohm 883 Basic IC plus chromatograph with a Metrohm 919 IC Autosampler plus and Metrosep C6 column, controlled via MagicNet 4.2 software. Analysis conditions: injection volume, 20 µL; eluent, 4 mM oxalic acid in Milli-Q water; flow rate, 0.9 mL/min; run time, 25 min. After each run, the column was flushed with 4 mM oxalic acid in Milli-Q water/MeCN (80:20 v/v; 0.7mL·min^{-1}) for 20 min, followed by re-equilibration with the eluent (5 min; 0.9 mL·min^{-1}) before the following injection. The calibration curve was obtained using $NH4^+$ standard solution (Sigma TraceCERT, 1000 ± 4 mg/L) diluted to 0.01, 0.05, 0.10, and 0.15 mM in H_2SO_4 (20 mM) in MeCN/Milli-Q water (5:95 v/v).

The average total amount of $NH4^+$ (mmol) for each sample (*S*, *C1*, *C2*) is reported in Table S4. Since the $NH4^+$ amounts in *C1* and *C2* are comparable and thus time-independent, they are attributed to N_2H_4 hydrolysis under acidic/aqueous conditions. The amount of NH_3 generated during the Fe-driven N_2H_4/MeCN condensation was thus derived as NH_4^+(*S*) - NH_4^+(*C1*) = 0.0022 ± 0.0003 mmol, corresponding to a 18 ± 2% yield based on the amount of Fe.

Conclusion

In this work, we report the synthesis and characterization of the first alkyl thiolate-supported Fe^{II}-N_2H_4 adduct, expanding the restricted catalog of reported Fe-hydrazine complexes with sulfur ligation. This mononuclear adduct, formed from dinuclear Fe^{II}-thiolate complexes bio-inspired from the Fe_2 unit in the FeMo-co,[3] is relevant in the field of nitrogenase-related biomimetic iron-sulfur chemistry. In particular, it may model features of a hypothetical enzymatic Fe-N_2H_4 intermediate within the FeMo-co, implicated in the *alternating* mechanism of biological nitrogen fixation.

The most significant outcome of this work is the formation of an Fe^{II}-acetohydrazonohydrazide complex generated from the reaction between N_2H_4 and CH_3CN mediated by Fe^{II}. The acetohydrazonohydrazide ligand formally arises from the condensation of a CH_3CN molecule with two hydrazine molecules. The proposed mechanism is based on the

electrophilic activation of CH_3CN by Fe^{II} followed by the nucleophilic attack of free hydrazine, resulting in the formation of two C-N bonds.

This iron-mediated C-N bond formation opens up possibilities for functionalizing hydrazine (or other reduced azo moieties) arising from N_2 fixation, potentially leading to the generation of nitrogen-containing chemicals derived from N_2.

To fully explore this potential, future work should focus on exploring the generality of this iron-mediated reaction with different nitriles and substituted hydrazines and tuning complex properties through ligand design. Equally important are assessing potential catalytic applications and conducting mechanistic studies to understand the factors driving this unexpected reactivity.

Supporting Information

Further spectroscopic data (^{1}H NMR, infrared) for **Fe_2^S/Fe_2^{ss}** before and after addition of N_2H_4. Quantification of $NH4^+$ formation by Ion Chromatography. Single-crystal X-ray diffraction data for **Fe^{N2H4}** and **Fe^{N2H4}·Fe^{N4C2H7}**. Deposition Number(s) <url href="https://www.ccdc.cam.ac.uk/services/structures?id=doi:10.1002/ejic.202400633">2379804 (for **Fe^{N2H4}·Fe^{N4C2H7}**), 2379805 (for **Fe^{N2H4}**)</url> contain the supplementary crystallographic data for this paper. These data are provided free of charge by the joint Cambridge Crystallographic Data Centre and Fachinformationszentrum Karlsruhe <url href="http://www.ccdc.cam.ac.uk/structures">Access Structures service</url>.

Acknowledgements

This work is supported by the French National Research Agency in the framework of the PUNCh program (ANR-21-CE07-0003-01), and of the “Investissements d'avenir” program (ANR-15-IDEX-02), the Labex ARCANE, CBH-EUR-GS (ANR-17-EURE-0003). The NanoBio ICMG (FR 2607), is acknowledged for providing facilities for NMR analysis (R. Sanahuges, N. Altounian) and support in single crystal X-Ray diffraction analysis (N. Altounian).

Keywords: bio-inspired chemistry, nitrogenase, metal-thiolate complexes, iron-hydrazine complexes, substrate activation

[1] a) O. Einsle, D. C. Rees, *Chem. Rev.* **2020**, *120*, 4969-5004; b) B. M. Hoffman, D. Lukoyanov, D. R. Dean, L. C. Seefeldt, *Acc. Chem. Res.* **2013**, *46*, 587-595; c) B. M. Hoffman, D. Lukoyanov, Z.-Y. Yang, D. R. Dean, L. C. Seefeldt, *Chem. Rev.* **2014**, *114*, 4041-4062; d) L. C. Seefeldt, Z.-Y. Yang, D. A. Lukoyanov, D. F. Harris, D. R. Dean, S. Raugei, B. M. Hoffman, *Chem. Rev.* **2020**, *120*, 5082-5106.

[2] a) Y. Roux, C. Duboc, M. Gennari, *ChemPhysChem* **2017**, *18*, 2606-2617; b) C.-H. Wang, S. DeBeer, *Chem. Soc. Rev.* **2021**, *50*, 8743-8761; c) M. J. Chalkley, M. W. Drover, J. C. Peters, *Chem. Rev.* **2020**, *120*, 5582-5636; d) Y. Tanabe, Y. Nishibayashi, *Angew. Chem. Int. Ed.* **2024**, *63*, e202406404.

[3] a) W. Kang, C. C. Lee, A. J. Jasniewski, M. W. Ribbe, Y. Hu, *Science* **2020**, *368*, 1381-1385; b) M. Rohde, D. Sippel, C. Trncik, S. L. A. Andrade, O. Einsle, *Biochemistry* **2018**, *57*, 5497-5504.

[4] B. M. Barney, J. McClead, D. Lukoyanov, M. Laryukhin, T.-C. Yang, D. R. Dean, B. M. Hoffman, L. C. Seefeldt, *Biochemistry* **2007**, *46*, 6784-6794.

[5] R. N. F. Thorneley, R. R. Eady, D. J. Lowe, *Nature* **1978**, *272*, 557-558.

[6] M. J. Dilworth, R. R. Eady, *Biochem. J* **1991**, *277*, 465-468.

[7] a) K. Tanifuji, Y. Ohki, *Chem. Rev.* **2020**, *120*, 5194-5251; b) I. Čorić, B. Q. Mercado, E. Bill, D. J. Vinyard, P. L. Holland, *Nature* **2015**, *526*, 96-99; c) S. E. Creutz, J. C. Peters, *J. Am. Chem. Soc.* **2015**, *137*, 7310-7313.

[8] J. L. Crossland, D. R. Tyler, *Coord. Chem. Rev.* **2010**, *254*, 1883-1894.

[9] a) D. Sellmann, Shaban Y. Shaban, Frank W. Heinemann, *Eur. J. Inorg. Chem.* **2004**, *2004*, 4591-4601; b) D. Sellmann, W. Soglowek, F. Knoch, G. Ritter, J. Dengler, *Inorg. Chem.* **1992**, *31*, 3711-3717; c) Y.-H. Chang, P.-M. Chan, Y.-F. Tsai, G.-H. Lee, H.-F. Hsu, *Inorg. Chem.* **2014**, *53*, 664-666; d) B. D. Stubbert, J. Vela, W. W. Brennessel, P. L. Holland, *Z. Anorg. Allg. Chem.* **2013**, *639*, 1351-1355; e) M. J. Zdilla, A. K. Verma, S. C. Lee, *Inorg. Chem.* **2008**, *47*, 11382-11390.

[10] L. Wang, M. Gennari, F. G. Cantu Reinhard, S. K. Padamati, C. Philouze, D. Flot, S. Demeshko, W. R. Browne, F. Meyer, S. P. de Visser, C. Duboc, *Inorg. Chem.* **2020**, *59*, 3249-3259.

[11] L. Wang, F. G. Cantu Reinhard, C. Philouze, S. Demeshko, S. P. de Visser, F. Meyer, M. Gennari, C. Duboc, *Chem. - Eur. J.* **2018**, *24*, 11973-11982.

[12] M.-A. Kopf, D. Varech, J.-P. Tuchagues, D. Mansuy, I. Artaud, *J. Chem. Soc., Dalton Trans.* **1998**, 991-998.

[13] a) G. Albertin, S. Antoniutti, E. Bordignon, S. Pattaro, *J. Chem. Soc., Dalton Trans.* **1997**, 4445-4454; b) L. D. Field, H. L. Li, S. J. Dalgarno, P. Jensen, R. D. McIntosh, *Inorg. Chem.* **2011**, *50*, 5468-5476; c) G. Albertin, S. Antoniutti, J. Castro, G. Gasparetto, *New J. Chem.* **2019**, *43*, 2676-2686.

[14] G. Albertin, S. Antoniutti, E. Bordignon, F. Chimisso, *Inorg. Chem. Commun.* **2001**, *4*, 402-404.

[15] K. Nakamoto, *Infrared and Raman Spectra of Inorganic and Coordination Compounds, Part B: Applications in Coordination, Organometallic, and Bioinorganic Chemistry*, 5 ed., John Wiley & Sons, **1997**.

[16] A. W. Addison, T. N. Rao, J. Reedijk, J. van Rijn, G. C. Verschoor, *J. Chem. Soc., Dalton Trans.* **1984**, 1349-1356.

[17] d. t. t. v. b. n. o. t. b. i. t. r. No significant changes over time can be observed by IR in the N-H stretching region.

[18] V. Y. Kukushkin, A. J. L. Pombeiro, *Chem. Rev.* **2002**, *102*, 1771-1802.

[19] C. Chen, W. Chen, H. Qiu, *Dalton Trans.* **2012**, *41*, 13405-13412.

[20] a) M. Gennari, D. Brazzolotto, J. Pecaut, M. V. Cherrier, C. J. Pollock, S. DeBeer, M. Retegan, D. A. Pantazis, F. Neese, M. Rouzieres, R. Clerac, C. Duboc, *J. Am. Chem. Soc.* **2015**, *137*, 8644-8653; b) D. Brazzolotto, M. Gennari, S. Yu, J. Pecaut, M. Rouzieres, R. Clerac, M. Orio, C. Duboc, *Chem. - Eur. J.* **2016**, *22*, 925-933; c) L. Wang, M. Zlatar, F. Vlahovic, S. Demeshko, C. Philouze, F. Molton, M. Gennari, F. Meyer, C. Duboc, M. Gruden, *Chem. - Eur. J.* **2018**, *24*, 5091-5094; d) L. Wang, M. Gennari, F. G. Cantu Reinhard, J. Gutierrez, A. Morozan, C. Philouze, S. Demeshko, V. Artero, F. Meyer, S. P. de Visser, C. Duboc, *J. Am. Chem. Soc.* **2019**, *141*, 8244-8253; e) M. Gennari, C. Duboc, *Acc. Chem. Res.* **2020**, *53*, 2753-2761; f) L. Sun, J. Gutierrez, A. L. Goff, D. Gatineau, T. A. Jackson, M. Gennari, C. Duboc, *ChemCatChem* **2024**, *n/a*, e202400270.

[21] a) D. Brazzolotto, F. G. Cantu Reinhard, J. Smith-Jones, M. Retegan, L. Amidani, A. S. Faponle, K. Ray, C. Philouze, S. P. de Visser, M. Gennari, C. Duboc, *Angew. Chem., Int. Ed.* **2017**, *56*, 8211-8215; b) K. Shen, M.

Gennari, C. Philouze, A. Velic, S. Demeshko, F. Meyer, C. Duboc, *Inorg. Chem.* **2024**, *63*, 9119-9128.
[22] G. M. Sheldrick*, Vol. 6.14*, **1998**.

Entry for the Table of Contents

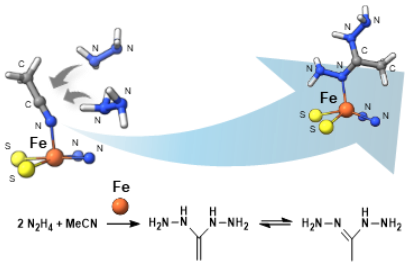

We report a unique iron(II)-hydrazine (N_2H_4) complex with alkyl thiolate ligands, potentially mimicking features of reduced nitrogenase intermediates in the biological N_2 reduction cycle. Unexpectedly, iron(II) mediates C-N bond formation between N_2H_4 and acetonitrile, yielding an acetohydrazonohydrazide complex. This result expands the reactivity landscape of iron-hydrazine complexes and suggests new pathways for N-N bond functionalization in nitrogen fixation processes.

Institute Twitter username: @DCMGrenoble